JOURNAL OF MATERIALS SCIENCE **34** (1999) 5893–5898

Hydrothermal precipitation of hydroxyapatite on anodic titanium oxide films containing Ca and P

H. ISHIZAWA, M. OGINO
Biomedical Engineering Laboratory, Department of Technological Development, Nikon Corporation, 1-10-1 Asamizodai, Sagamihara-shi, Kanagawa 228, Japan
E-mail: nba4686@oa.nikon.co.jp

Highly-crystallized hydroxyapatite (HA) can be precipitated during heat treatment in high-pressure steam at 300 °C on an anodic titanium oxide film containing Ca and P (AOFCP), which has been electrochemically formed on a titanium substrate prior to the hydrothermal treatment. Factors affecting the precipitation, such as a percentage of distilled water in the autoclave and additives in the AOFCP, were evaluated by scanning electron microscopy. Ca^{2+} and PO_4^{3-} ions were leached from the AOFCP into a water layer covering the film surface, and nucleate HA heterogeneously on the porous TiO_2 matrix of the AOFCP which was made by the ion leaching. The morphology of the precipitated crystals was significantly affected by the water volume ratio because the concentrations of the Ca^{2+} and PO_4^{3-} ions varied depending on the thickness of the water layer. The amount of the precipitation decreased on the AOFCP which was formed in the solution containing a small amount of Mg^{2+} ions or formed on Ti-6Al-4V alloy instead of titanium.

1. Introduction

Hydroxyapatite (HA) has many biological benefits, such as direct bonding to bone and enhancement of new bone formation around it. It has been demonstrated that dental and orthopaedic implants coated with HA show superior histological results to the uncoated ones [1–3]. Various methods as well as a plasma-spraying technique, which is most commonly used to coat HA on metallic implants, have been studied to produce HA coatings with high stability against mechanical fracture and dissolution in living tissue [4–11]. The stability of HA coatings is related to several factors such as crystallinity, composition, thickness and adhesive strength to the substrate. It is known that HA crystals with high crystallinity can be prepared by hydrothermal processing [11, 12]. Besides HA, crystalline thin films of $BaTiO_3$, $SrTiO_3$, and $CaTiO_3$ can be prepared on titanium and titanium-aluminum alloy by anodization under hydrothermal conditions [13, 14].

The present authors have developed a new method for forming highly-crystallized HA layers on titanium by anodization and subsequent hydrothermal treatment. It was found that an anodic titanium oxide film containing calcium (Ca) and phosphorus (P) (this film is abbreviated as AOFCP) was electrochemically formed on the anode substrate of titanium in an aqueous solution of dissolved calcium acetate (CA) and sodium β-glycerophosphate (β-GP) [15]. Spark discharges, which occur on a titanium anode under high electrolytic voltage with a large amount of heat generation, cause incorporation of Ca and P into the AOFCP from these electrolytes and crystallization of the TiO_2 matrix to an anatase phase simultaneously [16]. Near-stoichiometric HA microcrystals with high crystallinity are precipitated on the AOFCP formed under the particular electrolyte concentrations during hydrothermal treatment in high-pressure steam at 300 °C. As a result, thin HA layers of 1–2 μm thicknesses are synthesized on the AOFCP. The hydrothermally treated AOFCP attains very high adhesive strength to a titanium substrate and direct bonding between bone and the thin HA layer [17, 18]. However, little information has been obtained with respect to the precipitation of HA crystals. The factors affecting the nucleation and crystal growth of HA should be examined to clarify the precipitation mechanism. In this study, the effects of hydrothermal conditions and additives in the AOFCP were investigated by scanning electron microscopy.

2. Experimental

Commercially pure titanium was anodized up to 350V in an electrolytic aqueous solution containing β-GP (Kanto Chemical, Japan) and CA (Wako Pure Chemical Industries, Japan). The anodization was performed at current density of 50 mA/cm^2 using a regulated DC power supply (419A-630, Metronix, Japan). Three kinds of AOFCPs were formed in the solutions with different electrolyte concentrations and designated 01-15, 04-25, and 12-4. For example, 01-15 denotes the AOFCP formed in the electrolytic solution containing β-GP of 0.01 mol l^{-1} and CA of 0.15 mol l^{-1}. The bath temperature was kept at 20 °C by using a cooling equipment against heat generation caused by the anodization.

Exceptionally, titanium-6% aluminum-4% vanadium alloy (Ti-6Al-4V) was used as substrates instead of titanium, and the solution added magnesium acetate of 0.005 mol l^{-1} was used to form the Mg-doped AOFCP. Distilled water of 200 (15 vol %) or 600 mL (46 vol %) was put into an autoclave (volume: 1.3 L; Nitto-kouatsu, Japan). The anodized specimens were hanged in the center of the autoclave out of the distilled water, making the anodized surface vertical, and heated in high-pressure steam at 250 or 300 °C for 2 h. The autoclave indicated the same internal pressure of 8.5 MPa at both water volume ratios at 300 °C. Fig. 1 shows the flow chart of the experimental procedure to form the AOFCP and precipitate HA crystals. The morphology of the precipitated HA crystals was observed by scanning electron microscopy (SEM; DS-130, Topcon, Japan). The two-dimensional distributions of Ca and P in the film were measured on the carbon-coated film by an energy dispersive X-ray microanalysis (EDX; DX-4i, Philips, The Netherlands). The crystalline phases of the film were identified by an X-ray diffraction analysis (XRD; RAD-B system, Rigaku, Japan).

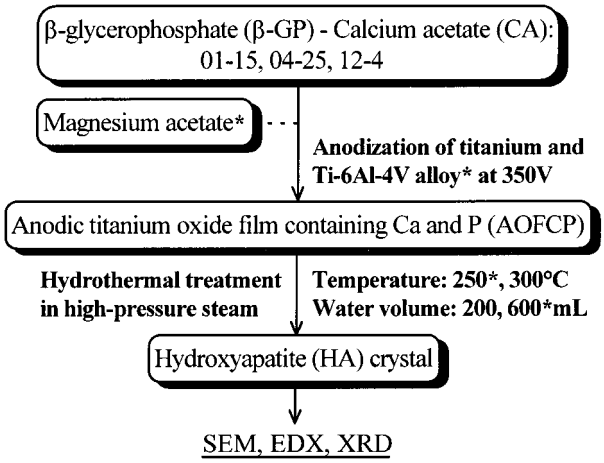

Figure 1 Experimental procedure for forming the AOFCP and HA crystals. (Asterisks indicate unstandard conditions, which are referred in the text whenever used.)

3. Results

3.1. Distributions of Ca and P in the AOFCP

The distributions of Ca and P in the hydrothermally treated and untreated 01-15 were examined by EDX. Ca and P were homogeneously dispersed in the untreated 01-15 (Fig. 2b). After hydrothermal treatment, the precipitated HA crystals incompletely covered the surface of 01-15 because its Ca and P contents were low (Fig. 2c). Ca and P were detected from the HA crystals, but hardly from the underlying AOFCP uncovered by the crystals (Fig. 2d). Thus, nearly all Ca and P were lost from the AOFCP after hydrothermal treatment. The surface of the hydrothermally treated 01-15 was observed under high magnification. The TiO_2 matrix of the underlying AOFCP on which HA crystals were precipitated had a porous microstructure with very fine pores, as shown in Fig. 3.

3.2. Hydrothermal temperature

The morphology of HA crystals precipitated on 01-15 at 250 °C was compared with that at 300 °C. At 300 °C,

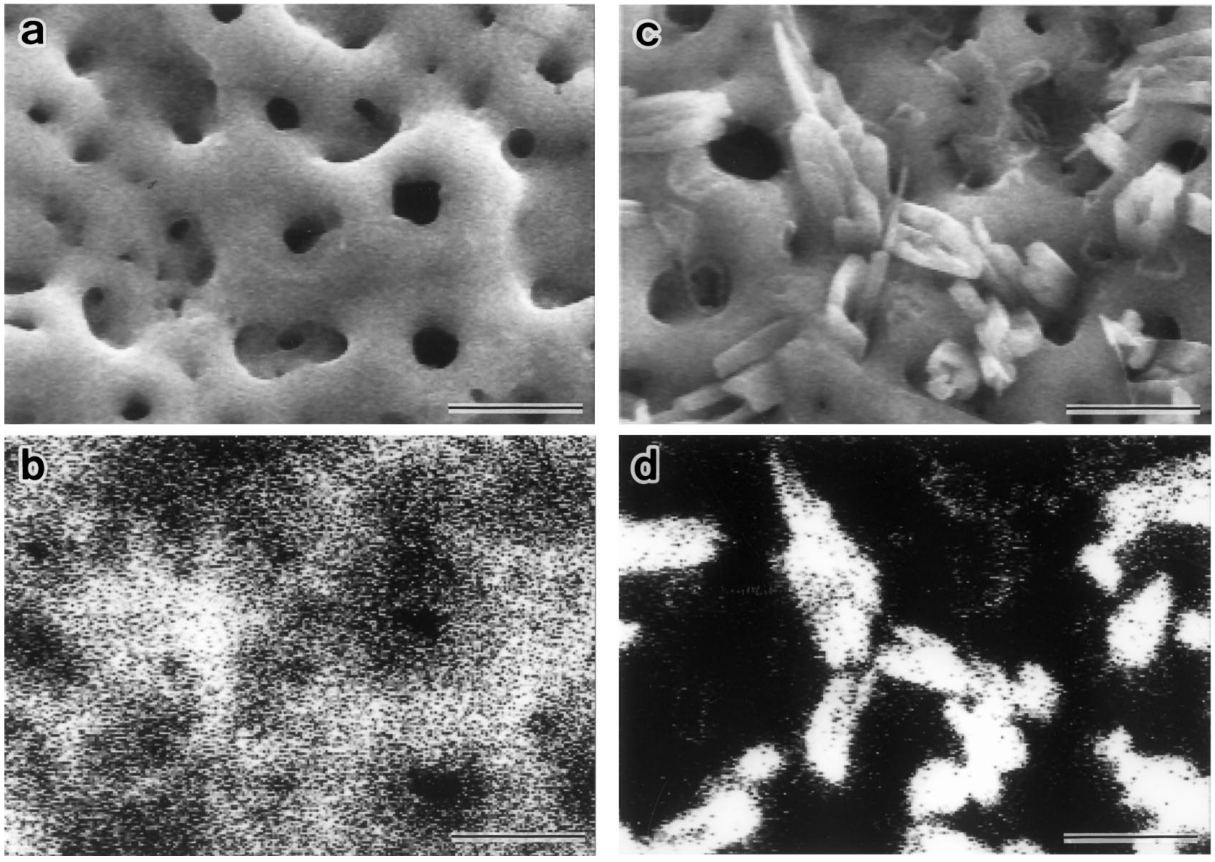

Figure 2 SEM micrographs of 01-15 (a) before and (c) after hydrothermal treatment. (b) and (d) show two-dimensional distributions of Ca for (a) and (c), respectively. P had a similar distribution to Ca. Bar = 5 μm.

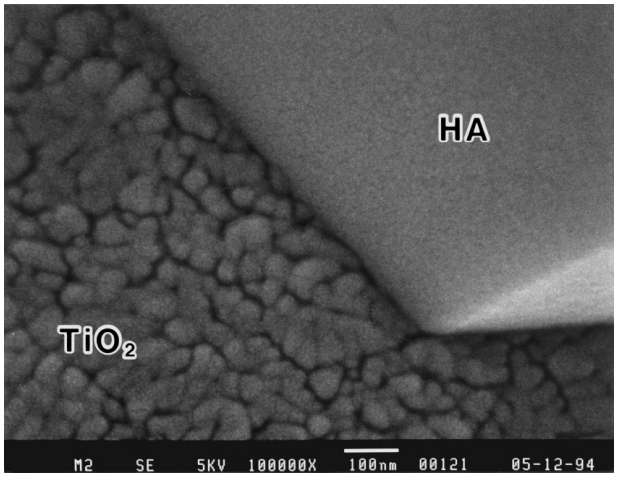

Figure 3 SEM micrograph of hydrothermally treated 01-15.

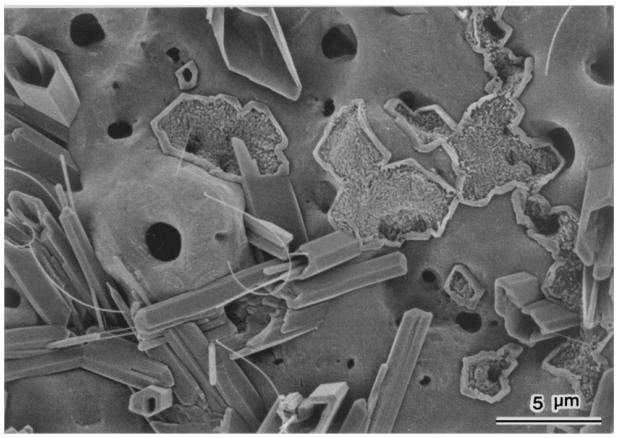

Figure 4 SEM micrograph of 01-15 treated hydrothermally at 250 °C.

every HA crystal had a columnar structure with sharp edges (Fig. 2c). But, HA crystals in an early stage of the growth, as well as hollow ones in the middle stage, were precipitated at 250 °C (Fig. 4). Such precursory HA crystals were encircled with walls, and the inside was filled with very fine crystals. The growth of the wall resulted in the HA crystal with hollow morphology. The SEM image showing the initial stage of the precipitation revealed that the HA crystals had grown not from the inside of the AOFCP but on the AOFCP surface.

3.3. Distilled water volume in an autoclave

The effect of the water volume ratio on the precipitation of HA was evaluated by altering the volume of distilled water put into the autoclave. 04-25 was heated in high-pressure steam at 15 and 46 vol % water. At 15 vol % water, a great many HA microcrystals were precipitated, completely covering the AOFCP surface (Fig. 5a). However, HA crystals with quite different morphology from the microcrystals were precipitated when the water volume ratio was increased to 46 vol %. The number of the crystals greatly decreased, but each crystal was highly developed into a form of long and upward hexagonal columns with sharp edges (Fig. 5b). Therefore, it was found that the water volume ratio significantly affected the precipitation of HA, especially the nucleation.

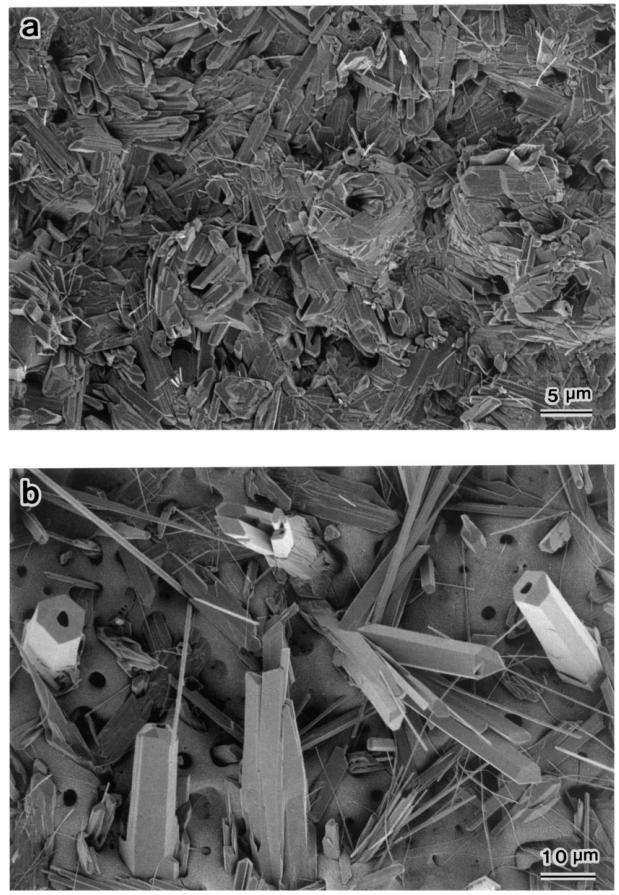

Figure 5 SEM micrographs of 04-25 treated hydrothermally at the water volume ratio of (a) 15 and (b) 46 vol %.

When a drain valve mounted on the base of the autoclave was opened at 300 °C, first water and after a while steam went out from the valve at both water volume ratios. Thus, the vapor phase in the autoclave was saturated with high-pressure steam of 8.5 MPa at 300 °C.

3.4. Mg-doping in the AOFCP

The electrolytic solution added magnesium acetate of 0.005 mol l^{-1} was used to form 04-25 doped with Mg. It was found that the precipitation of HA crystals obviously decreased in amount on the Mg-doped 04-25, compared with on the undoped 04-25 (Fig. 6). As shown in XRD patterns of Fig. 7a and b, the Mg-doped 04-25 showed lower peak height of HA than the undoped 04-25. The precipitation of HA crystals was inhibited by doping Mg in the AOFCP.

3.5. AOFCP formed on Ti-6Al-4V alloy

04-25 was formed on Ti-6Al-4V alloy in the same way as titanium, and then hydrothermally treated. The precipitated HA crystals significantly decreased in amount, similar to the case of the Mg-doped 04-25 (Fig. 8). The decrease was recognized also from the comparison between the XRD patterns for the films formed on titanium and Ti-6Al-4V alloy substrates (Fig. 7a and c). The color of the AOFCP formed on titanium was grayish-white, but that on Ti-6Al-4V was brown. The AOFCP formed on Ti-6Al-4V included small amounts of V and Al, which were detected by EDX.

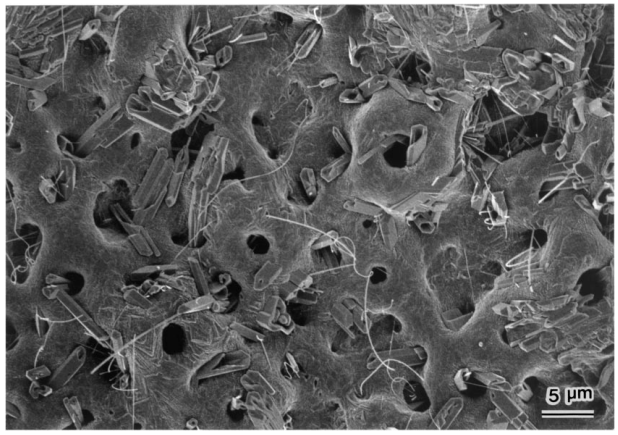

Figure 6 SEM micrograph of 04-25 formed in the electrolytic solution containing magnesium acetate of 0.005 mol l^{-1} and treated hydrothermally.

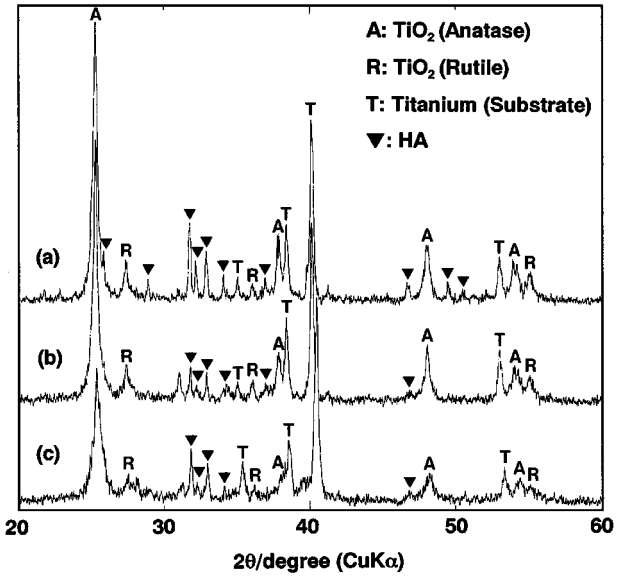

Figure 7 X-ray diffraction patterns of (a) 04-25, (b) Mg-doped 04-25 and (c) 04-25 formed on Ti-6Al-4V alloy, after hydrothermal treatment.

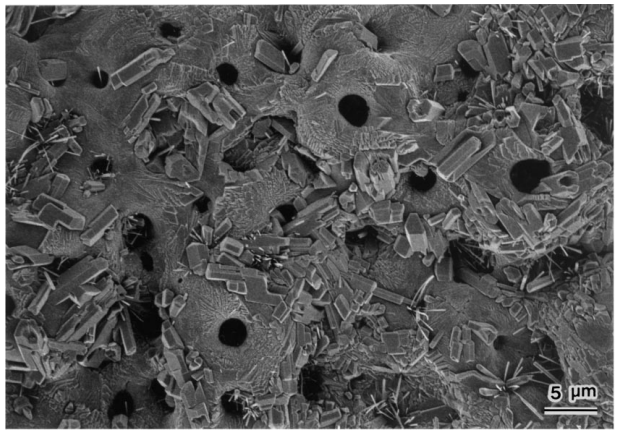

Figure 8 SEM micrograph of 04-25 formed on Ti-6Al-4V alloy and treated hydrothermally.

3.6. Electrolyte concentration

The precipitation amount of HA was compared between the hydrothermal treated 01-15, 04-25 and 12-4. The surface of 01-15 was incompletely covered with the HA microcrystals (Fig. 2c), but a continuous HA layer consisting of them was formed on 04-25 due to its higher Ca and P contents than 01-15 (Fig. 5a). On 12-4, which had further high Ca and P contents, numerous whisker-like HA crystals of about 5 μm length were precipitated perpendicularly to the AOFCP surface, as shown in Fig. 9. The precipitation amount increased with increasing the Ca and P contents of the AOFCP, that was, the electrolyte concentrations.

Figure 9 SEM micrograph of hydrothermally treated 12-4.

4. Discussion

From the EDX analysis for 01-15, it was found that the lost Ca and P to the AOFCP after hydrothermal treatment were used for the formation of HA crystals on the surface. This fact strongly suggests that Ca and P in the AOFCP are lost through leaching. Fig. 10 shows the schematic illustration of the precipitation mechanism of HA crystals on the AOFCP. The AOFCP surface appears to be moist with a water layer during hydrothermal treatment. It is thought that leaching of Ca^{2+} and PO_4^{3-} ions from the AOFCP, heterogeneous nucleation of HA on the porous TiO_2 matrix and finally crystal growth successively occur in the water layer. The porous TiO_2 matrix is probably made as a result of the ion leaching from the AOFCP. The leached Ca^{2+} and PO_4^{3-} ions are deposited onto the nucleation sites of the TiO_2 matrix and then nucleated HA with hydroxyl groups. As shown in Fig. 9, whisker-like HA crystals of about 5 μm length were precipitated on 12-4. Such HA crystals had been forced to grow vertically to the surface because the crystal growth along the surface was

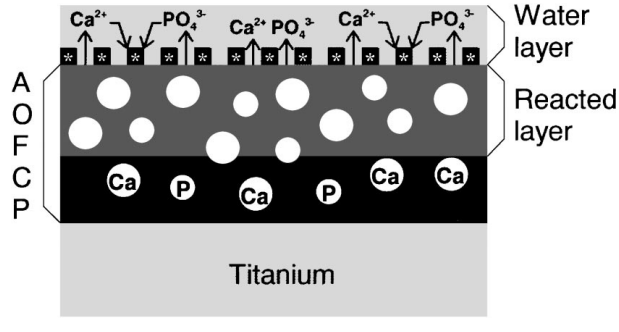

Figure 10 Schematic illustration showing the cross section of the AOFCP treated hydrothermally at the water volume ratio of 15 vol %. (Asterisks indicate the precipitated HA microcrystals).

obstructed by the adjacent crystals. The formation of the long crystals requires a water layer with an equivalent thickness to the crystal length. Thus, the water layer thickness at 15 vol % water appears to be at most 5 μm. The length of the highly-developed HA crystals precipitated at 46 vol % water was approximately 20–30 μm (Fig. 5b). Also in this case, the AOFCP surface seems to be covered with a water layer with an equivalent thickness to the length of the long crystal. The water layer thickness at 46 vol % water seems to be much higher than that at 15 vol % water.

Uniform nucleation of HA always occurred at 15 vol % water on the AOFCPs with any Ca and P contents, but never occurred at 46 vol % water. The difference in a water layer thickness is probably responsible for the distinctly different nucleation. At 15 vol % water, the concentrations of the leached Ca^{2+} and PO_4^{3-} ions are raised to highly enough to nucleate numerous HA in the thin water layer of about 5 μm thickness. However, the crystal growth of HA seems to be predominated rather than the nucleation in the thick water layer of 20–30 μm thickness with the low ion concentrations at 46 vol % water. As a result, the number of the nuclei is greatly reduced in comparison with the case at 15 vol % water. The nuclei that are once formed can be highly developed into the long HA crystals in compensation for the reduction in number.

A small amount of Mg^{2+} ions, as well as Ca^{2+} and PO_4^{3-} ions, appear to be leached from the Mg-doped 04-25 into the water layer. It is well known that Mg^{2+} ion inhibits calcium phosphate precipitation, similar to the other inhibitors such as Sr^{2+}, Zn^{2+} and Sn^{2+} [19]. It inhibits the crystal growth of HA by adsorbing onto the top of the precipitating crystal [20]. The decrease in amount of the HA crystals on the Mg-doped AOFCP is ascribed to the inhibition of the crystal growth due to the leached Mg^{2+} ions. If the AOFCP is formed in the electrolytic solution containing even a small amount of inhibitor ions, the ions will be leached into the water layer and inhibit the HA nuclei from growing to the crystals.

Li *et al*. described that TiO_2 gel as well as SiO_2 both induce abundant HA on the surface when immersed in a simulated body fluid containing Ca^{2+} and PO_4^{3-} ions, whereas, well-crystallized TiO_2, silica glass and quartz do not [21, 22]. As is well known, silicate bioactive materials, such as Bioglass® and glass-ceramic A-W, have the ability to form surface HA films spontaneously *in vivo* and *in vitro* [23, 24]. A SiO_2 gel layer, which is very suitable for nucleation sites of HA, is formed in the Bioglass® near the surface as a result of leaching of Na^+, Ca^{2+} and PO_4^{3-} ions, and a thin HA film is spontaneously formed on the gel layer. The ability of the AOFCP to precipitate HA crystals on itself is responsible for the porous TiO_2 matrix that seems to be made by the leaching of Ca^{2+} and PO_4^{3-} ions. However, the migration of these ions through the TiO_2 matrix of the AOFCP appears to be much more difficult than through a SiO_2 matrix of silicate bioactive materials, because no HA crystal was precipitated on the AOFCP under *in vivo* and *in vitro* conditions. Thus, the hydrothermal treatment under high temperature and high-pressure steam is required to make Ca^{2+} and PO_4^{3-} ions leach out from the AOFCP. The TiO_2 matrix had high crystallinity of an anatase phase after heating at 300 °C (Fig. 7). As found by Li *et al.*, well-crystallized TiO_2 leads to the difficulty of the heterogeneous nucleation of HA. It is thought that necessary activation energy for the HA nucleation on the TiO_2 matrix is greatly reduced by virtue of its porous microstructure. Such porous TiO_2 seems to be helpful to the HA nucleation although it has high crystallinity.

Small amounts of Al and V were involved in the AOFCP formed on a Ti-6Al-4V alloy substrate. The coloring of the AOFCP to brown is probably attributed to the formation of V_2O_5 in the AOFCP, because the color of V_2O_5, which assumes yellow or rust-brown, corresponds with that of the film. Small amounts of Al_2O_3 and V_2O_5 appear to be formed in the TiO_2 matrix by anodizing aluminum and vanadium as well as titanium of the alloy substrate, which are all so-called valve metals. It was reported that Al_2O_3 gel does not induce HA in a simulated body fluid containing Ca^{2+} and PO_4^{3-} ions, unlike SiO_2 and TiO_2 gel [22]. A small amount of Al_2O_3 contained in the TiO_2 matrix, also possibly V_2O_5, is unsuitable for the nucleation sites of HA. The difficulty of the nucleation on these oxides may lead to the less amount of the precipitation. The AOFCP without inhibitor ions and oxides against calcium phosphate precipitation must be hydrothermally treated at the water volume ratio of about 15 vol % to synthesize a continuous HA layer consisting of the precipitated microcrystals.

5. Conclusions

The precipitation mechanism of the HA crystals on the AOFCP was clarified. Leaching of Ca^{2+} and PO_4^{3-} ions from the AOFCP, heterogeneous nucleation of HA on the porous TiO_2 matrix and finally crystal growth successively occurred in a water layer covering the film surface during the hydrothermal treatment. The nucleation was significantly affected by the water volume ratio and inhibited by the additional oxides such as Al_2O_3 and V_2O_5 in the AOFCP formed on an anode substrate of Ti-6Al-4V. The crystal growth was suppressed on the AOFCP formed in the electrolytic solution containing a small amount of the inhibitor ions such as Mg^{2+}.

References

1. S. D. COOK, J. F. KAY, K. A. THOMAS and M. JARCHO, *Int. J. Oral maxillofac. Impl.* **2** (1987) 15.
2. *Idem., Clin. Orthop.* **232** (1988) 225.
3. K. DE GROOT, R. GEESINK, C. P. A. T. KLEIN and P. SEREKIAN, *J. Biomed. Mater. Res.* **21** (1987) 1375.
4. J. G. C. WOLKE, K. VAN DIJK, H. G. SCHAEKEN, K. DE GROOT and J. A. JANSEN, *ibid.* **28** (1994) 1477.
5. K. YAMASHITA, T. ARASHI, K. KITAGAKI, S. YAMADA and K. OGAWA, *J. Amer. Ceram. Soc.* **77** (1994) 2401.
6. K. HATA, T. KOKUBO, T. NAKAMURA and T. YAMAMURO, *ibid.* **78** (1995) 1049.
7. M. SHIRKHANZADEH, *J. Mater. Sci. Mater. Med.* **6** (1995) 90.
8. T. BRENDEL, A. ENGEL and C. RÜSSEL, *ibid.* **3** (1992) 175.

9. H. MONMA, *J. Ceram. Soc. Japan*. **101** (1993) 737.
10. A. A. CAMPBELL, G. E. FRYXELL, J. C. LINEHAN and G. L. GRAFF, *J. Biomed. Mater. Res*. **32** (1996) 111.
11. Y. FUJISHIRO, T. SATO and A. OKUWAKI, *J. Mater. Sci. Mater. Med*. **6** (1995) 172.
12. K. IOKU, M. YOSHIMURA and S. SOMIYA, *Nippon Kagaku Kaishi* (1988) 1565.
13. M. YOSHIMURA, in Materials Research Society Symposium Proceedings, Vol. 271, Better Ceramics through Chemistry [V] (Materials Research Society, Pittsburgh, PA, 1992) p. 457.
14. M. YOSHIMURA, W. URUSHIHARA, M. YASHIMA and M. KAKIHANA, *Intermetallics* **3** (1995) 125.
15. H. ISHIZAWA and M. OGINO, *J. Biomed. Mater. Res.* **29** (1995) 65.
16. *Idem., J. Mater. Sci.* **31** (1996) 6279.
17. *Idem., J. Biomed. Mater. Res.* **29** (1995) 1071.
18. H. ISHIZAWA, M. FUJINO and M. OGINO, *ibid*. **29** (1995) 1459.
19. B. N. BACHRA and H. R. A. FISCHER, *Calcif. Tissue Res.* **3** (1969) 348.
20. M. H. SALIMI, J. C. HEUGHEBAERT and G. H. NANCOLAS, *Langmuir* **1** (1985) 119.
21. P. LI, I. KANGASNIEMI, K. DE GROOT and T. KOKUBO, *J. Amer. Ceram. Soc*. **77** (1994) 1307.
22. P. LI, C. OHTSUKI, T. KOKUBO, K. NAKANISHI, N. SOGA and K. DE GROOT, *J. Biomed. Mater. Res.* **28** (1994) 7.
23. H. ISHIZAWA, M. FUJINO and M. OGINO, in "Handbook of Bioactive Ceramics," Vol. I, edited by T. Yamamuro, L. L. Hench and J. Wilson (CRC Press, Boca Raton, 1990) p. 115.
24. T. KOKUBO, S. ITO, Z. T. HUANG, T. HAYASHI, S. SAKKA, T. KITSUGI and T. YAMAMURO, *J. Biomed. Mater. Res*. **24** (1990) 331.

Received 20 February 1997
and accepted 20 April 1999